Chemical Bonding and Physical Properties of Yb_5Bi_3

Ying Liang[a,b], Raul Cardoso-Gil[a], Walter Schnelle[a], Marcus Schmidt[a], Jing Tai Zhao[b], and Yuri Grin[a]

[a] Max-Planck-Institut für Chemische Physik fester Stoffe, Nöthnitzer Str. 40, 01187 Dresden, Germany
[b] State Key Lab of High Performance Ceramics and Superfine Microstructures, Shanghai Institute of Ceramics, Chinese Academy of Sciences, Dingxi Road 1295, Shanghai 200050, P. R. China

Reprint requests to Prof. Dr. Yu. Grin. E-mail: juri.grin@cpfs.mpg.de

Z. Naturforsch. **2007**, *62b,* 935 – 940; received April 2, 2007

Dedicated to Prof. Dr. Bernard Chevalier on the occasion of his 60th birthday

The binary compound Yb_5Bi_3 was synthesized by reaction of the elements in a sealed Ta container. Its crystal structure was determined from single-crystal X-ray diffraction data: β-Yb_5Sb_3-type, space group *Pnma*, Pearson code *oP*32, $a = 12.6375(6)$, $b = 9.7243(4)$, $c = 8.4117(5)$ Å, $V = 1033.72(9)$ Å^3, $Z = 4$, $R_{gt}(F) = 0.028$, $wR_{ref}(F^2) = 0.069$, $T = 290$ K. Band structure calculations and analysis of the chemical bonding suggest mainly ionic interactions in the crystal structure and a possible presence of ytterbium in two valence states Yb^{2+} and Yb^{3+}. The magnetization measurements showed that at low temperatures Yb_5Bi_3 contains ytterbium exclusively in the $4f^{14}$ configuration without fluctuations to the Yb $4f^{13}$ configuration up to 400 K. From the Yb-L_{III} X-ray absorption spectroscopy data the effective valence of ytterbium was found to be 2.11 (89 % of Yb in $4f^{14}$ configuration).

Key words: Ytterbium, Bismuth, Intermetallic Compound, Chemical Bonding, Magnetism, Electrical Resistivity, X-Ray Absorption Spectroscopy

Introduction

Three types of crystal structures have been found for the binary R_5Bi_3 phases (R = rare earth metal). The compounds with the early rare earth elements La, Ce, Pr and Nd form crystal structures of the Mn_5Si_3-type [1] while the Y_5Bi_3-type crystal structure is found for the Dy, Ho, Er, Tm, and Y compounds [2 – 4]. Gd_5Bi_3 and Tb_5Bi_3 form polymorphs with both structure types mentioned above. The compound Eu_5Bi_3 crystallizes in the β-Yb_5Sb_3 structure [5] which is closely related to that of Y_5Bi_3 [6, 7]. The two latter types are isopointal and can be described as a three-dimensional framework formed by hexagonal columns $^1_\infty[BiR_6]$ parallel to [010]. A chain of alternating R and Bi atoms is situated within the hexagonal column.

The compound Yb_5Bi_3 was reported to crystallize either in the β-Yb_5Sb_3 structure type [5, 8], or in the Mn_5Si_3-type [9]. Later, Corbett *et al*. [10, 11] suggested that hydrogen should be a stabilizing factor for compounds with the β-Yb_5Sb_3-type crystal structure, and the compounds should be rather formulated as R_5Sb_3H. Thus, further work on Yb_5Bi_3 is worth to be carried out to investigate its properties and to clarify the divergence between the reported results. In the present paper, we report on the crystal structure of hydrogen-free Yb_5Bi_3 obtained from single crystal X-ray diffraction data. Ytterbium compounds are interesting not only for their diverse crystal structures but also for the varying valence states of the rare earth metal which may give rise to novel physical properties. Thus the electronic state of ytterbium was investigated in detail by measurements of magnetic susceptibility, X-ray absorption spectroscopy experiments, band structure calculations, and analysis of the chemical bonding in direct space.

Experimental Section

The sample with the composition Yb_5Bi_3 (sample **1**) was obtained by the direct reaction of ytterbium (HIREM, China, 99.9 %) and bismuth pieces (Chempur 99.9999 %) in an argon-filled glove box. Stoichiometric amounts of the metals were pressed to pellets and filled into tantalum crucibles (cleaned with dilute hydrochloric acid and heated at 1273 K for 12 h in a dynamic vacuum), which were sealed by arc welding. The crucibles were then sealed in evacuated quartz tubes for preventing oxidation at elevated temperatures. For

Table 1. Crystallographic data for Yb_5Bi_3.

Space group	*Pnma* (no. 62)
Unit cell parameters (powder data)	
a, Å	12.6375(6)
b, Å	9.7243(4)
c, Å	8.4117(5)
Unit cell volume, Å^3	1033.72(9)
Number of formula units per unit cell	4
Calculated density, g cm^{-3}	9.59
Radiation; wavelength, Å	AgK_α; 0.56087
Diffractometer; scan mode	Stoe-IPDS; φ scan
Absorption correction	numerical
Absorption coefficient, cm^{-1}	518.5
Mode of refinement	$F(hkl)$
Weighting scheme	unit
Extinction formalism; parameter	Sheldrick-II; 0.0022(1)
Number of refined parameters	44
$2\theta_{max}$, deg; $(\sin\theta/\lambda)_{max}$, Å^{-1}	44.62; 0.677
Number of measured reflections	9475
Number of unique reflections	1421
Number of reflections used in refinement	1264
Residual values	$R_{gt}(F) = 0.028$, $wR_{ref}(F^2) = 0.069$
Goodness of fit	1.083

the growth of single crystals, the sample was first heated to 1373 K within 12 h and held at that temperature for 2 h. Subsequently, the temperature was slowly reduced to 1173 K over a period of 24 h and held at that temperature for 7 d. Finally the tubes were quenched in ice water. The sample was easily separated from the tantalum crucibles, and no reaction of the sample with the crucible material was detected. Thermal analysis was carried out using a DTA apparatus STA 409C (Netzsch). For DTA measurements the sample was sealed in a tantalum ampoule and heated with a rate of 10 K min^{-1} in the temperature range 300 – 1773 K under flowing argon. The compound $Yb_5Bi_3H_{0.25}$ (sample **2**) was obtained using the method described above. However, the tantalum crucibles were not pre-heated in vacuum.

The quantitative determination of hydrogen was carried out by the carrier gas hot extraction method (TCH600, LECO) and detection of H_2O *via* IR absorption.

X-Ray powder diffraction data were collected on a Huber G670 Guinier Image-Plate Camera using CoK_α radiation (λ = 1.78896 Å) and pure Si (a = 5.43102 Å) as internal standard. The lattice parameters were refined by least-squares methods with the program package WINCSD [12].

Single crystals of Yb_5Bi_3 exhibiting metallic lustre were isolated from the bulk reaction product and sealed into glass capillaries. Diffraction data from a single crystal with the size of $0.054 \times 0.092 \times 0.126$ mm^3 were collected on a Stoe-IPDS diffraction setup with AgK_α radiation (λ = 0.56087 Å). The structure was solved by Direct Methods using the program SHELXS-97 [13] and refined with SHELXL-97 [14]. Numbers pertinent to the structure determination are summarized in Table 1.

Electrical conductivity was measured in a standard dc four-point setup on sample **1** between 4 and 320 K.

The magnetization of the bulk material (sample **1**) was measured in a SQUID magnetometer (MPMS-XL7, Quantum Design) in external fields between 100 Oe and 70 kOe at temperatures between 1.8 and 400 K. The sample was sealed in a quartz tube under helium atmosphere (500 mbar) in order to prevent oxidation.

The X-ray absorption spectrum (XAS) at the Yb-L_{III} threshold was recorded on sample **1** at the HASYLAB EXAFSII beamline E4 at DESY using a Si (111) double crystal monochromator. Yb_2O_3 was used as standard for the $4f^{13}$ (Yb^{3+}) configuration. To prevent oxidation the powdered sample was placed under argon in a beryllium-windows cell.

For quantum chemical calculations, the Stuttgart TB-LMTO-ASA program package [15] with an exchange correlation potential (LDA) according to Barth and Hedin [16] was used. The radial scalar-relativistic Dirac equation was solved to get the partial waves. The calculation within the atomic sphere approximation (ASA) includes corrections for the neglect of interstitial regions and partial waves of higher order [17]. In case of Yb_5Bi_3 the addition of empty spheres was not necessary. The following radii of atomic spheres were applied for calculations: r(Yb1) = 1.887 Å, r(Yb2) = 2.014 Å, r(Yb3) = 1.479 Å, r(Yb4) = 2.049 Å, r(Bi1) = 2.054 Å, r(Bi2) = 1.920 Å. A basis set of Yb(6s,5d,4f) and Bi(6s,6p) orbitals was applied for the calculations; the Yb(6p) and Bi(6d,5f) orbitals were downfolded. The electron localizability indicator (ELI, Y) was chosen as an appropriate tool to investigate the atomic interactions in real space. ELI was evaluated according to ref. [18], with the help of a program package [15] with an ELI module already implemented. To gain more detailed insight into the chemical bonding, the topology of ELI was analyzed using the program BASIN [19].

Results and Discussion

The analysis of the X-ray powder diffraction pattern of sample **1** confirmed the formation of Yb_5Bi_3 crystallizing in the β-Yb_5Sb_3-type. No evidence of any crystalline impurity was observed within the detection limit of the method. The microstructure of the material is characterized by large grains (100 – 200 μm) of the main phase and very small point-like inclusions. The EDXS measurements revealed the composition $Yb_{5.08(15)}Bi_{2.92(18)}$, being well in agreement with the results of the crystal structure determination within one e.s.d. Thermal analysis (DTA) of the annealed sample **1** have revealed a clear endothermic peak on heating at 1645 K corresponding to the peritectic decomposition of Yb_5Bi_3 found, *e.g.*, at 1630 K in ref. [9].

Table 2. Atomic coordinates and displacement parameters (Å^2) in the crystal structure of Yb_5Bi_3.

Atom	Site	x	y	z	U_{eq}	U_{11}	U_{22}	U_{33}	U_{12}	U_{13}	U_{23}
Bi1	8*d*	0.32877(3)	0.01385(4)	0.06705(5)	0.0106(1)	0.0088(2)	0.0107(2)	0.0124(2)	0.0006(1)	0.0018(1)	0.0011(1)
Bi2	4*c*	0.48305(4)	1/4	0.57948(6)	0.0099(1)	0.0091(2)	0.0093(2)	0.0113(3)	0	−0.0014(2)	0
Yb1	8*d*	0.07387(4)	0.04409(5)	0.19517(6)	0.0134(1)	0.0159(2)	0.0103(2)	0.0140(2)	−0.0000(2)	−0.0039(2)	−0.0010(2)
Yb2	4*c*	0.00560(5)	1/4	0.53446(8)	0.0112(2)	0.0085(3)	0.0136(3)	0.0114(3)	0	0.0005(2)	0
Yb3	4*c*	0.22999(5)	1/4	0.81864(9)	0.0130(2)	0.0092(3)	0.0151(3)	0.0146(3)	0	−0.0019(2)	0
Yb4	4*c*	0.28860(5)	1/4	0.34877(8)	0.0136(2)	0.0093(3)	0.0175(3)	0.0139(3)	0	−0.0021(2)	0

Table 3. Interatomic distances (Å) in Yb_5Bi_3.

Atoms	Distance	Atoms	Distance	Atoms	Distance
Bi1–Yb2	3.3161(6)	Bi2 – 2Yb1	3.1054(5)	Yb1–Bi2	3.1054(5)
Yb2	3.3226(6)	Yb4	3.1313(9)	Bi2	3.2656(7)
Yb4	3.3387(7)	Yb3	3.2362(8)	Bi1	3.4083(6)
Yb3	3.3463(6)	Yb2	3.2598(9)	Bi1	3.4095(6)
Yb3	3.4079(6)	2Yb1	3.2656(7)	Yb2	3.5915(8)
Yb1	3.4083(6)	Yb3	3.7782(9)	Yb4	3.6114(7)
Yb1	3.4095(6)			Bi1	3.6988(7)
Yb4	3.4864(6)	Yb3–Bi2	3.2362(8)	Yb2	3.7894(7)
Yb1	3.6988(7)	2Bi1	3.3463(6)	Yb1	3.8734(10)
		2Bi1	3.4079(6)	Yb3	3.9244(7)
Yb2–Bi2	3.2598(9)	Yb2	3.6957(9)	Yb1	4.0046(10)
2Bi1	3.3161(6)	Yb2	3.7088(9)	Yb4	4.1404(8)
2Bi1	3.3226(6)	Bi2	3.7782(4)		
2Yb1	3.5915(8)	2Yb1	3.9244(7)	Yb4–Bi2	3.1313(9)
Yb3	3.6957(9)	Yb4	4.0212(10)	2Bi1	3.3387(7)
Yb3	3.7088(9)	Yb1	4.2348(8)	2Bi1	3.4864(6)
2Yb1	3.7894(7)			2Yb1	3.6114(7)
Yb4	3.9027(9)			Yb2	3.9027(9)
				Yb3	4.021(1)
				2Yb1	4.1404(8)
				Yb2	4.232(1)

To determine the presence of hydrogen in Yb_5Bi_3 as suggested by Corbett *et al*. [10], chemical analysis was carried out. No hydrogen was found within the detection limit (< 80 ppm by mass). Furthermore, sample **2** with the composition $Yb_5Bi_3H_{0.25}$ was obtained without the special treatment of the reaction containers in order to get rid of hydrogen. The lattice parameters refinement for sample **2** gave a = 12.6113(5), b = 9.7317(4), c = 8.4124(3) Å and V = 1032.45(7) Å^3, which match well the results of Corbett *et al*. [11] but are significantly larger than those of the hydrogen-free sample **1** (Table 1). This result shows that hydrogen can be easily incorporated into Yb_5Bi_3 but it is not necessary for the stabilization of the β-Yb_5Bi_3-type crystal structure of this compound.

The final values of the atomic coordinates and the displacement parameters in the crystal structure of Yb_5Bi_3 are summarized in Table 2, while Table 3 presents the interatomic distances. The Bi atoms occupy two crystallographically independent positions (8*d* and 4*c*) in space group *Pnma*. The coordination

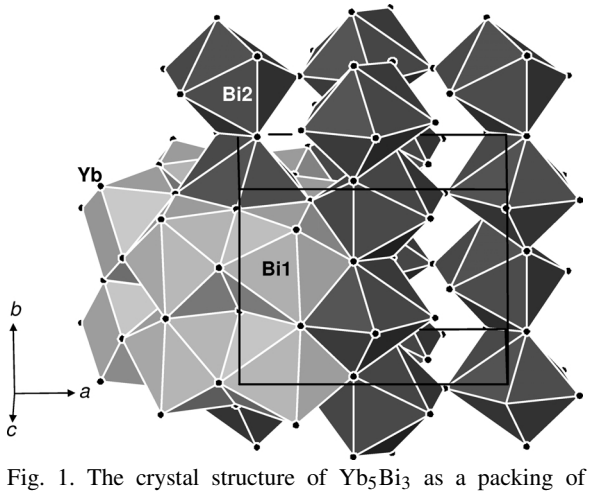

Fig. 1. The crystal structure of Yb_5Bi_3 as a packing of [Bi1Yb$_9$] (light grey) and [Bi2Yb$_8$] polyhedra (dark grey).

sphere of Bi1 can be described as a distorted tricapped trigonal prism (c.n. = 9) and that of Bi2 as a distorted bicapped trigonal prism (c.n. = 8). Layers of six-membered rings parallel to (010) are built up by the [Bi1Yb$_9$] polyhedra sharing faces. They are stacked along [010] by sharing the trigonal faces of the prisms. The remaining space is filled by [Bi2Yb$_8$] polyhedra sharing edges and forming chains along [010]. The chains are linked by common corners in the (010) plane. The resulting three-dimensional framework can be described as the arrangement of two interpenetrating frameworks consisting of the Bi1 and Bi2 polyhedra (Fig. 1).

The band structure calculation for Yb_5Bi_3 was performed using the structural data obtained from the diffraction experiment. The electronic density of states (DOS, Fig. 2) show fully occupied Bi *s* and *p* bands together with the Yb *s* band located at lower energy which may be interpreted within a classical Zintl scheme by charge transfer from ytterbium to bismuth. For this case, the total electronic balance may be written as

$$(Yb^{2+})_5(Bi^{3-})_3 \cdot e^- . \qquad (1)$$

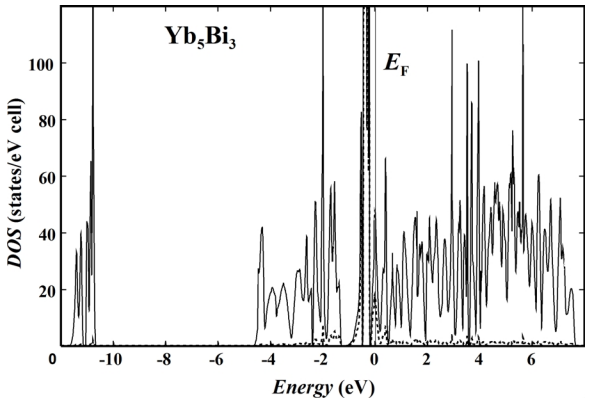

Fig. 2. Electronic density of states for Yb_5Bi_3. Total DOS is shown as full line, the dashed line represents the $4f$ contributions of ytterbium. The Fermi level is positioned at E = 0 eV.

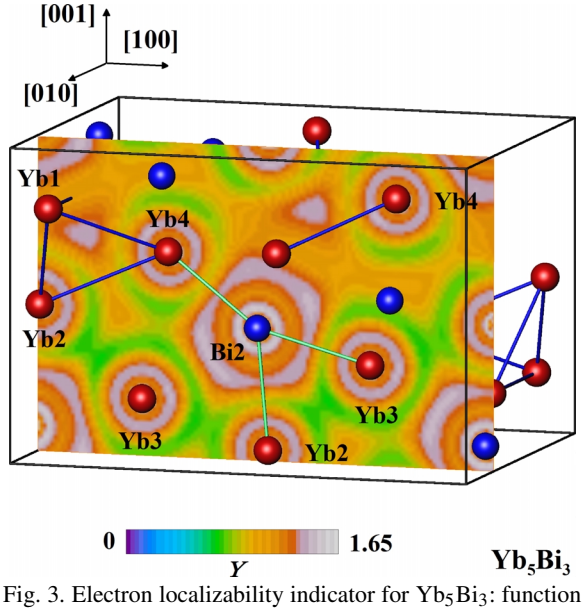

Fig. 3. Electron localizability indicator for Yb_5Bi_3: function distribution at y = 1/4. The shortest Bi2–Yb distances are shown in light green, the $(Yb1)_2(Yb2)(Yb4)$ tetrahedra with the ELI maxima in the center is indicated with blue lines (for colour see online version).

The small amount of additional excess electrons seems to be a stabilizing factor for the crystal structure of the β-Yb_5Bi_3-type. The final mechanism of such stabilization (additional two- and multi-centre bonds or more delocalized interactions) is still under discussion. However it has already been shown that excess electrons (as compared with the Zintl count) contributed by the cation are necessary to stabilize the crystal structures of so-called polar Zintl phases [20]. Because of the lack of a model for the stabilization mechanism, the necessary amount of excess electrons can be estimated only indirectly. The lower limit is given by the electron balance (1). For the upper limit one may use the fact that, in case of $Al_{0.9}B_2$ and $Mg_{0.95}B_2$ [21, 22], *ca.* $0.23e^-$ per each cation appear to be necessary for the stabilization of the corresponding structural pattern. Taking this into account, the electron balance may be written as

$$(Yb^{2+})_{4.85}(Yb^{3+})_{0.15}(Bi^{3-})_3 \cdot 1.15\ e^-. \qquad (2)$$

This requires a partial oxidation of ytterbium and correlates with the fact that the partially filled Yb $4f$ band located just around the Fermi level (Fig. 2) suggests a possible valence instability of Yb^{2+} ($4f^{14}$).

In the course of hydrogenation, the excess electron may be used for internal reduction and bonding of the hydrogen atoms, forming hydrides with the possible counts being either $(Yb^{2+})_5(Bi^{3-})_3(H^{1-})$ or $(Yb^{2+})_{4.85}(Yb^{3+})_{0.15}(Bi^{3-})_3(H^{1-}) \cdot 0.15\ e^-$ for the balances (1) and (2), respectively.

The picture of the predominant ionic interaction in the crystal structure of Yb_5Bi_3 was confirmed by the bonding analysis with the electron localizability indicator. The ELI distribution around the ytterbium atoms is nearly spherical (Fig. 3) and shows 5 atomic shells. The sixth one is not observed and the electrons appear to be transferred to the bismuth substructure. In the vicinity of the bismuth positions six shells are observed. The sixth one shows deviations from the spherical distribution, but is still closed around the nucleus (*cf.* Bi2 in Fig. 3). No distinct maxima are found between the ytterbium and the bismuth atoms in agreement with the ionic bonding picture (*cf.* the shortest distances between the Bi2 atom and its neighbors, shown in light green in Fig. 3). An additional maximum of ELI is observed inside the $(Yb1)_2(Yb2)(Yb4)$ tetrahedron (blue in Fig. 3). It reveals the excess electrons contributing to a special four-centre interaction within the ytterbium substructure in accord with the above electronic balance. The positions of the local maxima of the electron localization function or of the electron localizability indicator were shown to be very suitable for the hydrogen incorporation [23]. Upon full occupation of these positions the chemical composition of the hydride should be Yb_5Bi_3H in agreement with the electron balances (1) and (2) shown above.

The electrical resistivity $\rho(T)$ of sample **1** increases with temperature from the residual resis-

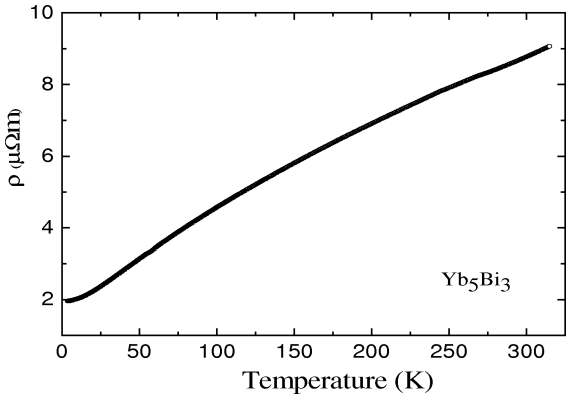

Fig. 4. Electrical resistivity $\rho(T)$ of polycrystalline Yb_5Bi_3 (sample **1**).

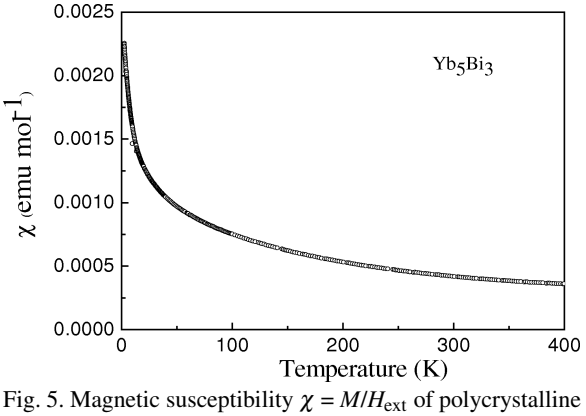

Fig. 5. Magnetic susceptibility $\chi = M/H_{ext}$ of polycrystalline Yb_5Bi_3 (sample **1**, H_{ext} = 10 kOe).

tivity ρ_0 = 2 $\mu\Omega$ m to ρ = 9 $\mu\Omega$ m at 300 K (Fig. 4), thus Yb_5Bi_3 shows a "bad metallic behaviour" ($\rho(300\ \mathrm{K}) > 1\ \mu\Omega$ m) in agreement with the results of electronic band structure calculations yielding an distinct electronic density of states at the Fermi level.

The magnetic susceptibility $\chi = M/H_{ext}$ of Yb_5Bi_3 *vs*. temperature is shown in Fig. 5. It can only be satisfactorily described by a Curie-Weiss law $C/(T + \Theta)$ together with a temperature-independent term χ_0. A fit based on this model results in μ_{eff} = 0.8 μ_B, Θ = −48 K, and $\chi_0 = +0.22 \times 10^{-3}$ emu mol^{-1} (per formula unit). Taking the free ion-effective moment for Yb^{3+}, the sample contains ≈ 1 % of Yb in the $4f^{13}$ configuration (Yb^{3+}). This would give an electron balance $(Yb^{2+})_{4.95}(Yb^{3+})_{0.05}(Bi^{3-}) \cdot 1.05\ e^-$ in astonishingly good agreement with the bonding analysis (*cf.* electron balance (2)) and partially occupied Yb ($4f$) states in the band structure. On the other hand, due to the large negative Θ value, the Yb^{3+} contribution more probably stems from a secondary phase with a phase content of ≈ 1 % (too little to be detected by XRD). Thus, at low temperatures, Yb_5Bi_3 contains ytterbium exclusively in the $4f^{14}$ configuration. Fluctuations to the Yb $4f^{13}$ configuration are not visible up to 400 K. No upturn of $\chi(T)$ at high temperatures, as it is typical for, *e. g.*, the ICF model [24], is observed for Yb_5Bi_3. The obtained χ_0 value corrected by the sum of the diamagnetic increments (-169×10^{-6} emu mol^{-1}) can be interpreted as a Pauli susceptibility χ_P, which corresponds to an electronic density of states $N(E_F) \approx 12$ states eV^{-1} per formula unit in fair agreement with the calculated ∼ 5 states eV^{-1} per formula unit. No phase transitions were observed at low temperatures.

The X-ray absorption spectrum at the Yb-L_{III} edge (ambient conditions) confirms the primary finding of the magnetic susceptibility measurements. Two peaks corresponding to $4f^{14}(Yb^{2+})$ and $4f^{13}(Yb^{3+})$ are observed (Fig. 6). The large amount of the $4f^{13}$ configuration is somehow in contradiction with the magnetization results. A presence of ytterbium oxide in such large amounts, which was often found for intermetallic compounds in the past, can be ruled out considering the preparation and sample handling. Deconvolution of the spectrum using the program XASWIN [25] leads to an effective valence of 2.11 (89 % of Yb $4f^{14}$), suggesting the electronic balance $(Yb^{2+})_{4.45}(Yb^{3+})_{0.55}(Bi^{3-})_3 \cdot 1.55\ e^-$, which gives a larger amount of excess electrons than suggested from the bonding analysis, but tendentially is still in agreement with the theoretical considerations.

Conclusions

The binary phase β-Yb_5Bi_3 was synthesized and its crystal structure was solved and refined from single crystal X-ray diffraction data (structure type β-Yb_5Sb_3). The additionally obtained hydride phase $Yb_5Bi_3H_{0.25}$ confirmed the ease of incorporation of hydrogen into Yb_5Bi_3, but the necessity of hydrogen for the stabilization of the β-Yb_5Sb_3-type crystal structure could be ruled out. Band structure calculations and analysis of the chemical bonding suggest mainly ionic interactions within the crystal structure of Yb_5Bi_3 and a possible presence of ytterbium in two valence states according to the electronic balance $(Yb^{2+})_{4.85}(Yb^{3+})_{0.15}(Bi^{3-})_3 \cdot 1.15\ e^-$. From the mag-

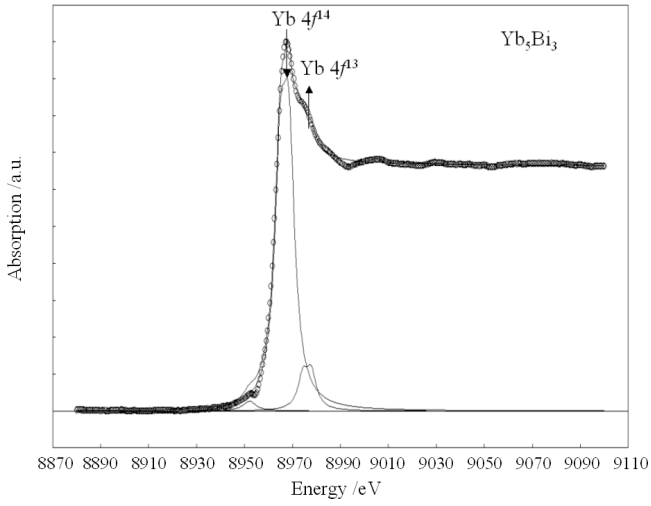

Fig. 6. X-Ray absorption spectrum of Yb_5Bi_3. Two main contributions ($4f^{13}$ and $4f^{14}$) are shown together with a pre-edge peak at lower energy.

netization measurements, at low temperatures Yb_5Bi_3 contains ytterbium exclusively in the $4f^{14}$ configuration, and no fluctuations to the Yb $4f^{13}$ configuration were found up to 400 K. Yb-L_{III} X-ray absorption spectroscopy reveals for ytterbium the effective valence of 2.11 (89 % of Yb in $4f^{14}$ configuration).

Acknowledgements

The authors would like to thank Ms. S. Müller for DTA, Dr. G. Auffermann and Mrs. A. Völzke for chemical analysis, Mr. R. Koban for susceptibility measurements, Mrs. M. Eckert for EDXS measurements, and Mr. S. Hückmann for collecting the powder diffraction data.

[1] K. Yoshihara, J. B. Taylor, L. D. Calvert, J. G. Despault, *J. Less-Common Met*. **1975**, *41*, 329.
[2] F. A. Schmidt, O. D. McMasters, R. R. Lichtenberg, *J. Less-Common Met*. **1969**, *18*, 215.
[3] S. P. Yatsenko, E. I. Hladyschewsky, K. A. Tschuntonow, Ya. P. Yarmolyuk, Yu. N. Hryn, *J. Less-Common Met*. **1983**, *91*, 21.
[4] M. Drzyzga, J. Szade, *J. Alloys Compd.* **2001**, *321*, 27.
[5] J. B. Taylor, L. D. Calvert, Y. Wang, *J. Appl. Crystallogr*. **1979**, *12*, 249.
[6] Y. Wang, E. J. Gabe, L. D. Calvert, J. B. Taylor, *Acta. Crystallogr*. **1976**, *B32*, 1440.
[7] G. D. Brunton, H. Steinfink, *Inorg. Chem.* **1971**, *10*, 2301.
[8] G. Borzone, R. Ferro, N. Parodi, A. Saccone, *Gazz. Chim. Ital*. **1995**, *125*, 263.
[9] T. F. Maksudova, P. G. Rustamov, O. M. Aliev, *J. Less-Common Met*. **1985**, *109*, L19.
[10] E. A. Leon-Escamilla, J. D. Corbett, *J. Alloys Compd.* **1994**, *206*, L15.
[11] E. A. Leon-Escamilla, J. D. Corbett, *J. Alloys Compd.* **1998**, *265*, 104.
[12] L. G. Akselrud, P. Yu. Zavalij, Yu. Grin, V. K. Pecharsky, B. Baumgartner, E. Wölfel, *Mater. Sci. For*. **1993**, *133 – 136*, 335.
[13] G. M. Sheldrick, SHELXS-97, Program for the Solution of Crystal Structures, University of Göttingen, Göttingen (Germany) **1997**.
[14] G. M. Sheldrick, SHELXL-97, Program for the Refinement of Crystal Structures, University of Göttingen, Göttingen (Germany) **1997**.
[15] O. Jepsen, O. K. Andersen, Program TB-LMTO-ASA (version 4.7), Max-Planck-Institut für Festkörperforschung, Stuttgart (Germany) **1999**.
[16] U. Barth, L. Hedin, *J. Phys*. **1972**, *C5*, 1629.
[17] O. K. Andersen, *Phys. Rev*. **1975**, *B12*, 3060.
[18] M. Kohout, *Int. J. Quantum Chem*. **2004**, *97*, 651.
[19] M. Kohout, BASIN (version 2.3), Max-Planck-Institut für Chemische Physik fester Stoffe, Dresden (Germany) **2001**.
[20] R. Nesper, *Prog. Solid State Chem*. **1990**, *20*, 1.
[21] J. Schmidt, W. Schnelle, Yu. Grin, R. Kniep, *Solid State Sci*. **2003**, *5*, 535.
[22] U. Burkhardt, V. Gurin, F. Haarmann, H. Borrmann, W. Schnelle, A. Yaresko, Yu. Grin, *J. Solid State Chem*. **2004**, *177*, 389.
[23] A. Savin, R. Nesper, S. Wengert, T. Fässler, *Angew. Chem*. **1997**, *109*, 1892.
[24] B. C. Sales, D. K. Wohlleben, *Phys. Rev. Lett*. **1975**, *35*, 1240.
[25] L. Akselrud, Yu. Grin, Program XASWIN, Max-Planck-Institut für Chemische Physik fester Stoffe, Dresden (Germany) **2004**.